JOURNAL OF CATALYSIS 125, 411–420 (1990)

Mechanism of Poisoning of the V_2O_5/TiO_2 Catalyst for the Reduction of NO by NH_3

J. P. CHEN AND R. T. YANG[1]

Department of Chemical Engineering, State University of New York, Buffalo, New York 14260

Received January 17, 1990; revised April 2, 1990

Alkali metals are among the strongest poisons to the V_2O_5/TiO_2 catalyst for selective catalytic reduction of NO by NH_3. The strength of the poison is directly related to its basicity. SO_2, in contrast, promotes the activity. The chemisorbed NH_3 on the catalyst is predominantly NH_4^+, bonded to the Brønsted acid site of V–OH. A direct correlation exists between the amount of chemisorbed ammonia and the activity of the poison-doped catalyst. Furthermore, dehydroxylation of the catalyst by heat treatment eliminates its activity, which is restored rapidly by exposure to water vapor. Extended Hückel molecular orbital (EHMO) calculation was performed on a model V_2O_5/TiO_2 surface. The extraction energy for proton from the V–OH group and the net charge of H in the V–OH group are used as indices for Brønsted acidity. The EHMO results show decreases in the Brønsted acidity by the addition of alkali metals, and the order of the decrease follows the order of the basicity of the alkali metal. SO_2, in contrast, increases the Brønsted acidity. These results indicate that the Brønsted acid sites are the active sites for the reaction. Alkali metals poison the catalyst by decreasing its Brønsted acidity. SO_2 promotes the activity by increasing the Brønsted acidity.

INTRODUCTION

Selective catalytic reduction (SCR) of nitrogen oxides with ammonia on V_2O_5/TiO_2 catalyst is of increasing commercial interest. A comprehensive review of this subject has been made recently by Bosch and Janssen (*1*). Two main mechanisms have been suggested in the extensive literature. The first mechanism is an Eley–Rideal mechanism proposed by Murakami and co-workers (*2*) which requires dual sites of $V^{5+}=O$ and $V^{4+}—OH$. NH_3 is adsorbed on the dual sites forming NH_4^+, upon which NO is adsorbed forming an activated adduct. Upon decomposition of the activated species, N_2, H_2O, and V—OH are formed. The V—OH site can be reoxidized to $V^{5+}=O$ by either O_2 or bulk $V^{5+}=O$ species. This mechanism was used to interpret the following stoichiometry:

$$4NO + 4NH_3 + O_2 \rightarrow 4N_2 + 6H_2O. \quad (1)$$

It was further proposed that the density of the $V^{5+}=O$ sites on a V_2O_5 catalyst could be determined from the amount of N_2 produced in the initial portion of the pulse (of NH_3 + NO)–response experiment (*3, 4*). The basis of the experiment was the assumption that, upon a pulse of NH_3 + NO, an initial sharp peak in the N_2 production was due to the reaction on the dual sites, converting the V=O group to V—OH, which had to be oxidized slowly to form V=O by lattice oxygen. The pulse–response experiment was later performed by Bosch *et al.* (*5*) on a V_2O_5/TiO_2 catalyst with monolayer vanadia, where bulk $V^{5+}=O$ was not available. A constant low rate of N_2 production was observed after the initial response during subsequent, repeated NH_3/NO pulses. This low rate was interpreted by a reduction–oxidation mechanism which was supported by various experimental evidence (*6, 7*). In this mechanism, NH_3 reduces the $V^{5+}=O$ site, which is reoxidized by NO (and N_2O) to produce N_2 and regenerate the V=O site. This mechanism was

[1] To whom correspondence should be addressed.

0021-9517/90 $3.00

used to interpret the following stoichiometry:

$$6NO + 4NH_3 \rightarrow 5N_2 + 6H_2O. \quad (2)$$

Extensive literature on the structures of V_2O_5 supported on various supports is also available and has been reviewed by Bosch and Janssen (*1*). It is clear that both dual V=O/V—OH sites and V=O sites not adjacent to V—OH are abundant on V_2O_5/TiO_2 under the SCR reaction conditions, and both the Eley–Rideal and redox mechanisms should contribute to the reaction.

Importance of the V^{5+}=O sites in the SCR reaction was stressed in publications by Murakami *et al.* after 1980 (*1*). However, extensive experimental evidence has been shown for a lack of correlation between the SCR activity and the density of V^{5+}=O sites (*8–10*). Experimental evidence has also been shown that the V—OH groups alone are the active sites (*10, 11*). This is also consistent with the early IR results that the NH_4^+ (i.e., NH_3 chemisorbed on Brønsted sites) is the predominant species at the SCR reaction temperature (*2, 12*).

A major concern in practical applications of SCR has been the deactivation of the catalyst. Catalysts can be deactivated by a variety of phenomena among which poisoning is perhaps the least understood (*13, 14*). Poisoning is, however, the major reason for deactivation in SCR. Although scattered results on the poisoning of the SCR catalyst have been published, they appear to be confusing and little is understood on the subject. Poisoning by compounds of alkali metals has been identified (*15–17*), but the mechanism of poisoning remains unclear. Kasaoka *et al.* (*16*) reported that, in the absence of SO_2, the severity of poisoning follows the order KCl > NaCl > K_2SO_4 > Na_2SO_4, and all poison effects vanished in the presence of SO_2. Shikada and Fujimoto reported promoting effects of NaCl, Na_2SO_4, Li_2SO_4, and other alkali salts on V_2O_5/TiO_2 in SCR (*17*).

A comprehensive study on poisoning of V_2O_5/TiO_2 in SCR was undertaken in this work. Alkali metal oxides were identified as the strongest poisons, whereas SO_2 and halides exhibited promoting effects. This paper reports these effects, along with a rational, theoretical interpretation. An insight into the mechanism of the SCR reaction is also gained from the poisoning and promoting effects of the additives.

EXPERIMENTAL

The catalyst support was prepared from TiO_2 powder (P25, Degussa) by a densification procedure (*18*). The mixture of 1 : 1.75 (by weight) TiO_2 : distilled water was dried at 60°C (in air) for 24 hr and at 120°C for 72 hr before crushing and sieving to collect the 20- to 32-mesh fraction. The collected fraction was subsequently calcined at 600°C first in air for 1 hr and then in helium for 6 hr. The N_2 BET surface area (measured with a Quantasorb, Quantachrome Corp.) of the calcined support was 30.6 m^2/g.

The catalyst was impregnated by incipient wetness with an aqueous solution of NH_4VO_3 in oxalic acid. The impregnated catalyst was first dried at 120°C for 3–4 hr, followed by calcination at 500°C in O_2 for 3 hr. The amount of V_2O_5 was kept at 5% (by weight) TiO_2. The BET surface area of the supported catalyst was 26.3 m^2/g. Based on the results published in the literature, this catalyst contained well beyond a complete monolayer of surface vanadia which is coordinated to the TiO_2 (*8, 18*) and additional V_2O_5 crystallites (*19*).

The poison-doped catalysts were prepared by impregnation via incipient wetness with the precursor solutions of corresponding salts on the 5% V_2O_5/TiO_2 catalyst. The precursor solutions for Li_2O, Na_2O, K_2O, Rb_2O, and Cs_2O were, respectively, LiAc, $NaNO_3$, KNO_3, RbAc, and CsAc. The impregnated catalysts were dried at 120°C for 3–4 hr and then calcined to decompose the precursor salts. The calcination was carried out at 450°C for 4 hr. The doping of the poisons did not significantly decrease the

surface area, e.g., 26.1 m^2/g for 0.6% K_2O dopant.

The catalyst activity was measured by the conversion of NO through a packed-bed reactor. The reactor was a 2-cm-i.d., 30-cm-long quartz tube, equipped with a thermocouple well (which was inserted into the catalyst bed) and a gas preheating section. Catalyst pellets (2 cm^3) were charged in the reactor. The reactor temperature was controlled by a programmable temperature controller (CN 2012K, Omega). The NO/NO_x concentration was measured by a chemiluminescent $NO/NO_2/NO_x$ analyzer (Model 10, Thermo Electron Corp.). A phosphoric acid scrubber was used to remove NH_3 from the gas mixture before it entered the chemiluminescent analyzer.

The gases were supplied by Linde Division with the following purities: N_2 (O_2-free grade, <0.5 ppm O_2), NH_3 (anhydrous, 99.99%), NO (>98.5%), SO_2 (99.9%), and O_2 (ultrahigh purity, >99.99%). The gas mixture composition and flow rate were controlled by an FM 4575 Mass Flow Blending System (Linde Division).

The reactor system was also used for measuring the amounts of NH_3 chemisorption (at 200°C) on catalysts. The influent to the packed bed (0.5-ml catalysts were used) was 1000 ppm NH_3 in N_2, and the effluent was directly fed to the chemiluminescent analyzer. A high-temperature converter in the analyzer converted NH_3 by the reaction $NH_3 + O_2 \rightarrow NO_x + H_2O$ so the concentration of NH_3 could be measured. The chemisorbed amount was the difference between the influent and effluent.

IR spectra were measured with a Perkin–Elmer 727B spectrometer. The catalysts, 5% V_2O_5/TiO_2 and those doped with K_2O, were treated at 500°C in N_2 for 2 hr, cooled to the room temperature, and then exposed to NH_3 for 10 min. The samples were subsequently purged in an N_2 atmosphere for 20 min and pelletized with KBr at a ratio of 1 : 40 (catalyst : KBr) for IR measurement.

TABLE 1

Atomic Orbital Parameters and Diagonal Hamiltonian Energies (H_{ii}) Used in EHMO Calculation

Atom	Orbital	Orbital exponent	H_{ii} (eV)		
			s	*p*	*d*
H	1*s*	1.3	−13.6		
O	2*s*,2*p*	2.275	−32.6	−14.8	
Li	2*s*,2*p*	0.650	−5.40	−3.50	
Na	3*s*,3*p*	0.733	−5.10	−3.00	
K	4*s*,4*p*	0.874	−3.80		
S	3*s*,3*p*	1.817	−20.0	−13.3	
V	4*s*,4*p*,3*d*	1.20(*s*), 0.75(*p*) 4.75(d_1), 1.5(d_2)			0.456(c_1) 0.752(c_2)

MOLECULAR ORBITAL CALCULATION AND MODEL SELECTION

To help understand the nature of the active sites and the poisoning mechanism, the extended Hückel molecular orbital (EHMO) method was employed to perform calculations on a model active surface. The EHMO method and details of the computer program used in this work have been described elsewhere (*20, 21*). The parameters used in the calculations are given in Table 1.

It has been shown from a number of studies that the surface of the monolayer V_2O_5 supported on TiO_2 (anatase) is predominantly (010) face (or the basal plane) due to the epitaxy between this face and TiO_2 (*22–25*). This is the case even with high loadings of V_2O_5; e.g., Murakami *et al.* (*40*) noted that with 30–40 layers of V_2O_5, about 80% of the face was (010) face. The fractions of the (010) face of V_2O_5 supported on alumina or on unsupported V_2O_5 are considerably less than that supported on TiO_2 (anatase). Moreover, the V=O species are exposed only on the (010) face (*26*), and these species are abundant on V_2O_5/TiO_2 [e.g., (*1*)]. For these reasons, the (010) face of V_2O_5 was chosen as the model for the EHMO calculation. The structure of the (010) face and the lattice parameters are shown in Fig. 1. The lattice parameters are taken from Enjalbert and Galy (*27*). The

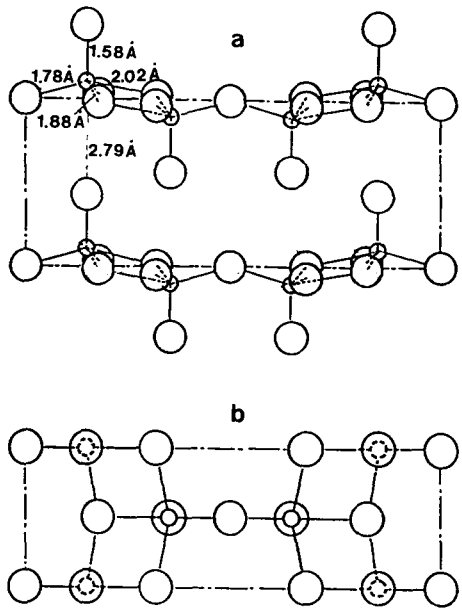

FIG. 1. (a) Structure of V_5O_5 as seen from the (001) plane; small circles denote V atoms and large circles, O atoms. Numbers are V–O distances in Å. (b) Projection of the structure on the (010) plane.

layers of the (010) plane are linked by weak V–O interactions with a bond distance of 2.79 Å.

There are two vacant V^{5+} sites on the model surface shown in Fig. 1b, which are filled by hydroxyl groups from the dissociation of water. To facilitate discussion, a simplified version of the (010) face, with the added OH groups, is shown in Fig. 2. The simplified version represents the central portion of Fig. 1b. All EHMO calculations, however, were performed with all atoms shown in Fig. 1b. The dopants (Li, Na, etc.) were located at the positions denoted A_1–A_4 (Fig. 2). These sites are oxygen sites which are more liable to interact with the alkali metals and SO_2, as compared to the other surface sites which are OH groups. Cs and Rb were not included in the EHMO calculation because their atomic orbital parameters are not available. Two groups were used in the calculation: one with two sites occupied (A_1 and A_2), and the other with all four sites occupied (A_1 to A_4). The distance between the dopant and oxygen was taken as that in the bulk crystal, as given below: 1.82 Å for Li–O (*28*), 2.35 Å for Na–O (*29*), 2.62 Å for K–O (*30*), 1.53 Å for SO_2–O (obtained by geometry optimization to obtain the minimum energy).

RESULTS AND DISCUSSION

Activity vs Dopant Amount

The catalyst activity for the SCR reaction may be represented by the rate constant. The reaction is first-order with respect to NO (*1, 2, 41*),

$$r = -\frac{1}{W}\frac{d[\mathrm{NO}]}{dt} = k[\mathrm{NO}]^1[\mathrm{NH_3}]^0, \quad (3)$$

where r = rate, W = amount of catalyst, and k is the rate constant. Under the flow conditions in the packed-bed reactor, the first-order rate constant may be obtained from the fractional conversion of NO(X) as

$$k = -\frac{F_0}{[\mathrm{NO}]_0 W}\ln(1 - X), \quad (4)$$

where F_0 is the inlet molar flow rate of NO and $[NO]_0$ is the inlet molar concentration.

The first series of experiments involved the 5% V_2O_5/TiO_2 pellets in two different size fractions: 20–32 mesh and 100–200 mesh. The temperature-programmed reaction results, given as NO conversion versus temperature, showed peak conversions at

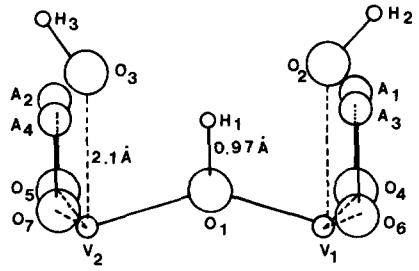

FIG. 2. Simplified model of (010) face of V_2O_5 (from Fig. 1a with dopant). All atoms in Fig. 1b are used in EHMO calculation. A_1–A_4 denote alkali metals or SO_2.

approximately 300°C. (A decline in conversion at higher temperature was due to the oxidation of ammonia.) However, no differences were observed in the TPR results for the two different-size fractions. Moreover, the space velocity was 15,000 hr^{-1} for both experiments. The rate constant calculated from Eq. (4) did not increase upon increase in the flow rate. These results confirmed that the measured reaction rate was without the influence of diffusion limitations.

Although the reaction order is well established for the undoped catalyst, a series of experiments were performed to check if the reaction is indeed first order (with respect to NO) on the poison-doped catalysts. Different amounts of the catalyst 1.08% K_2O/5% V_2O_5/TiO_2 (atomic M/V = 0.4) were used in the packed-bed reactor under the following conditions: 500 cm^3/min (NTP), 1000 ppm NH_3 and NO, 2% O_2, balance N_2, 300°C. The following conversions (X) versus catalyst amount (W) were obtained: 44.6% with 2.019 g, 38.5% with 1.615 g, 31.5% with 1.211 g, 22.5% with 0.807 g. The corresponding values for $[NO]_0W/F_0$ were 0.471, 0.371, 0.283, and 0.188. An integral analysis of these results yields a linear relationship between $-\ln(1 - X)$ and $[NO]_0W/F_0$, which indicates that the reaction is also first order on the poison-doped catalyst.

Figure 3 summarizes the data on the first-order rate constants at 300°C for the 5% V_2O_5/TiO_2 catalyst doped with various amounts of alkali metal oxides. The dopant concentration was expressed as the atomic ratio of alkali/vanadium. The results clearly demonstrate that the strength of the poison is directly related to its basicity, following the order $Cs_2O > Rb_2O > K_2O > Na_2O > Li_2O$. The alkali/V atomic ratios for 50% deactivation are 0.07 (Cs/V), 0.12 (Rb/V), 0.14 (K/V), 0.31 (Na/V), and 0.58 (Li/V). These results indicate that deactivation by the alkali metals not only is due to site blockage, but is related to the electron-donating ability of the dopant which may have a long-range influence.

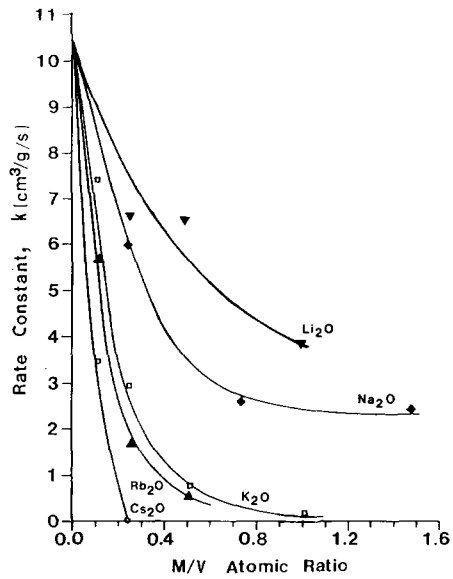

FIG. 3. First-order rate constant (k) for SCR reaction on 5% V_2O_5 (wt)/TiO_2 doped with various amounts of alkali metal oxides, where M = Li–Cs. Reaction conditions: $[NH_3]$ = [NO] = 1000 ppm, $[O_2]$ = 2%, N_2 = balance, T = 300°C, GHSV = 15,000 hr^{-1}.

Chemisorption of NH_3 on Undoped and Doped Catalysts

Chemisorption was used as a probe to indicate the amount of active sites on the poison-doped catalysts. The chemisorption was measured at 200°C with 1000 ppm NH_3 in N_2 at atmospheric pressure. The results are shown in Fig. 4 for alkali metals in different amounts. The results in Figs. 3 and 4 show a direct correspondence between SCR activity and NH_3 chemisorption.

To further understand the nature of the acid sites responsible for NH_3 chemisorption, IR spectra of the chemisorbed NH_3 on the 5% V_2O_5/TiO_2 catalyst and on a K_2O-doped catalyst were measured, as shown in Fig. 5. The strong band at 1415 cm^{-1} is due to NH_4^+, and this result is in agreement with previous work on NH_3 chemisorption at SCR temperatures (*1, 2, 12, 31*).

The IR band at 1415 cm^{-1} corresponds to NH_3 chemisorbed on Brønsted acid sites,

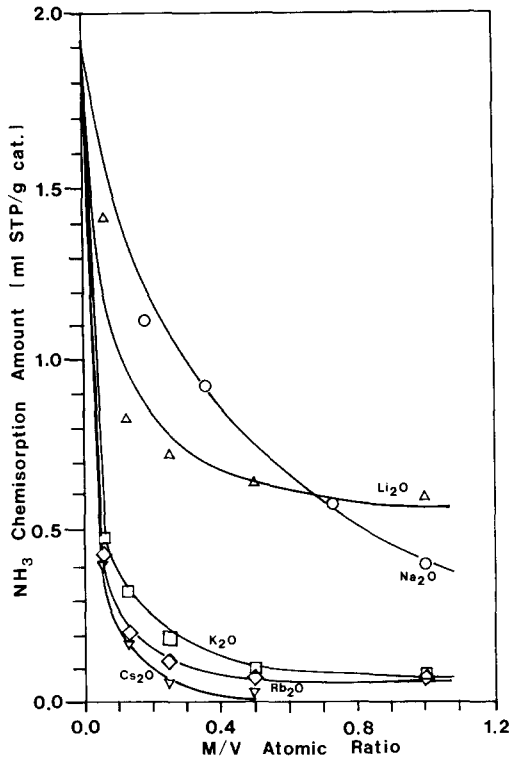

FIG. 4. Amount of NH_3 chemisorption at 200°C on 5% V_2O_5 (wt)/TiO_2 doped with alkali metals (M). 2.0 ml STP/g is equivalent to 0.16 mole NH_3/mole V on the surface.

V–OH (*32*). The very weak band at 1640–1660 cm^{-1} may be assigned to NH_3 chemisorbed on Lewis acid sites on V_2O_5 (*32*). The results in Fig. 5 indicate that the predominant sites on the V_2O_5/TiO_2 catalyst are Brønsted acid sites. Results in Fig. 5 also show that the amount of ammonia bonded to the Brønsted acid sites decreases with the amount of potassium doped on the catalyst, whereas the amount of NH_3 adsorbed on the Lewis acid sites remains unaffected. The results on chemisorption (Fig. 4) are consistent with the IR results (Fig. 5). For example, on a 0.32% K_2O (K/V = 0.13) catalyst, ammonia chemisorption is decreased to 0.33 cm^3 STP/g (from 1.93 cm^3 STP/g on the undoped catalyst), consistent with the large decrease in the IR band at 1415 cm^{-1}. The amount of 1.93 cm^3 STP/g (on the undoped catalyst) is equivalent to approximately 0.25 mole NH_3 per mole of surface V atoms.

The correlation between SCR activity and NH_3 chemisorption indicates that Brønsted acidity is essential for the reaction, and the NH_3 chemisorbed on the Brønsted acid sites is responsible for the reaction. Furthermore, the effect of the doped alkali metals is to lower the Brønsted acidity or to decrease the proton-donating ability of the Brønsted acid sites.

Effect of SO_2

The effect of SO_2 on the SCR reaction is a complex one due to the homogeneous reactions forming ammonium bisulfate (*33*) and sulfate (*15*) which deposit on the catalyst surface and block the micropores. Alumina is not used as the support due to the formation of aluminum sulfate which also

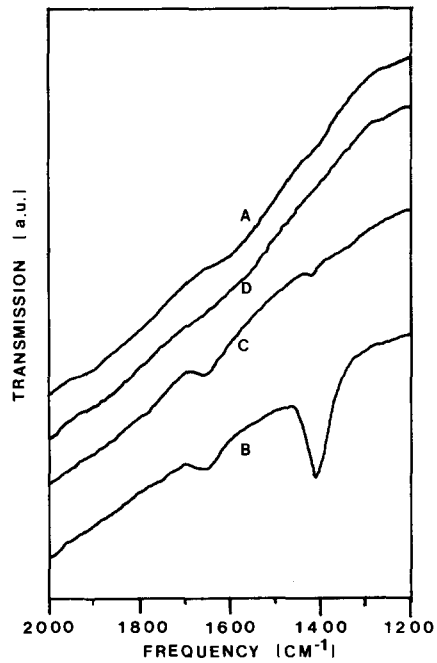

FIG. 5. IR spectra of (A) 5% V_2O_5/TiO_2 after treatment at 500°C in N_2 for 2 hr; (B) the same catalyst after NH_3 adsorption at room temperature followed by purge in dry N_2; and catalysts doped with 0.32% (wt) K_2O (C) and 2.5% K_2O (D), following the same NH_3 treatment.

TABLE 2

Effect of SO_2 (1000 ppm) on the SCR Activity of Undoped and Doped Catalysts[a]

	5% V_2O_5/TiO_2	0.16% Li_2O doped	0.64% Li_2O doped
Without SO_2			
NO conversion (%)	98.0	91.4	76.3
Rate constant, k (ml/g/sec)	10.39	6.52	3.82
With SO_2			
NO conversion (%)	99.2	94.0	98.5
Rate constant, k (ml/g/sec)	12.82	7.47	11.08

[a] $[NH_3] = [NO] = 1000$ ppm, $[O_2] = 2\%$, N_2 = balance, $T = 300°C$, GHSV = 15,000 hr^{-1}.

causes pore blockage (*34*). On the contrary, scattered reports of a promoting effect by SO_2 on SCR activity have been published (*35*).

The effects of SO_2 on the V_2O_5/TiO_2 catalyst and those doped with Li_2O are shown in Table 2. SO_2 has a promoting effect on both undoped and alkali-doped catalysts. Similar effects of SO_2 have also been observed for catalysts doped with Na_2O, K_2O, and Rb_2O (but not shown here).

For the alkali-doped catalysts, surface sulfates are undoubtedly formed in the presence of SO_2. It is known that metal sulfates are solid acids with Brønsted acid sites (*36*). Hence it is likely that the promoting effect of SO_2 is due to the enhancement of the Brønsted acidity.

Results of EHMO Calculation

The simplified model shown in Fig. 2 will be used for discussion, although the entire model in Fig. 1b was used for the EHMO calculation. The model contains OH groups on the vacant vanadium sites and H on the O bridge in V–O–V.

The abstraction energy for a proton, E_{H^+}, from the surface hydroxyl group and the net charge, Q_{H^+}, of the H atom in the hydroxyl group were calculated with the EHMO program (*20, 21*). The E_{H^+} and Q_{H^+} values provide useful information on the strength of the Brønsted acidity. The results are shown in Table 3, which includes the (010) face substrate and that doped with alkali atoms of SO_2 in A_1–A_4 positions.

There are three OH groups on the simplified model (Fig. 2): one bridge (O_1O_1) and two terminal (O_2H_2 and O_3H_3). (The subscripts are indices marked on Fig. 2.) The net charge on the bridge H is 0.33 and its abstraction energy is 5.33 eV. The corresponding values for the two terminal OH groups are 0.39 for net charge and 4.67 eV for proton abstraction energy. Comparison of these values indicates that the terminal V–OH groups have a stronger Brønsted acidity than the bridge V–OH–V group.

Upon the addition of alkali metals (Li, Na, and K), the hydrogen net charges are decreased whereas the proton abstraction energies are increased. Thus, the Brønsted acidity is decreased by the alkali metals. Moreover, the efficacy for lowering the Brønsted acidity follows the order K > Na > Li. This result on the lowering of the Brønsted acidity coincides with the decrease in SCR activity (as indicated by the rate constant, k) shown in Fig. 3.

The addition of SO_2 on the (010) face results in an opposite effect; the hydrogen net charges are increased and the proton abstraction energies are decreased. This result

TABLE 3

EHMO Results of the Net Charge of H on V–OH, Q_{H^+}, and Abstraction Energy of H^+ from V–OH, E_{H^+}, on the (010) Face of V_2O_5[a]

Model	System, dopant	Net charge, Q_{H^+} (e)			Abstraction energy, E_{H^+} (eV/H atom)		
		H_1	H_2	H_3	H_1^+	H_2^+	H_3^+
1	Substrate	0.330	0.390	0.390	5.35	4.67	4.67
2	2 Li	0.326	0.369	0.360	5.37	4.83	4.83
3	4 Li	0.326	0.350	0.350	5.37	4.94	4.94
4	2 Na	0.321	0.352	0.356	5.39	5.00	5.00
5	4 Na	0.318	0.340	0.340	5.42	5.14	5.14
6	2 K	0.318	0.338	0.330	5.37	5.05	5.05
7	4 K	0.311	0.315	0.315	5.39	5.29	5.29
8	2 SO_2	0.318	0.488	0.488	5.51	3.9	3.90
9	4 SO_2	0.310	0.618	0.618	5.67	2.31	2.31

[a] See Fig. 1 for model and Fig. 2 for dopant and H locations. With two alkali atoms, A_1 and A_2 are occupied, with four, A_1–A_4 are occupied.

indicates that SO_2 increases the Brønsted acidity. The increase in the Brønsted acidity is in agreement with the promoting effect of SO_2 (Table 2).

As noted in the foregoing, the Brønsted acidity of the terminal V–OH groups (on the vacant V sites) is considerably greater than that on the bridge V–OH–V group (Table 3). Moreover, the Brønsted acidity of the bridge group appears to be less influenced by the addition of alkali or SO_2. This result indicates that the terminal V–OH groups are the active sites for the SCR reaction.

Effect of Dehydroxylation

The importance of the surface OH groups in the SCR reaction is further demonstrated by three identical experiments with the only difference in sample pretreatment. The 5% V_2O_5/TiO_2 catalyst was used in these experiments. The results are compared in Fig. 6. In run A, the catalyst was directly heated to the reaction temperature (300°C) and the reactant mixture was subsequently admitted. In run B, the sample was heated to 650°C in dry He, held at 650°C in dry O_2 for 2 hr, and cooled to 300°C for the reaction. Run C differed from run B only in the addition of 2.2% water vapor in the reactant mixture.

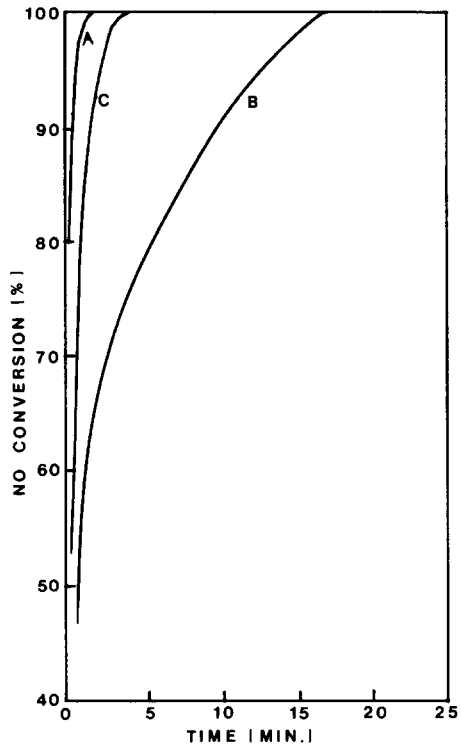

FIG. 6. Effect of heat treatment (dehydroxylation) and water (rehydroxylation) on activity with 5% V_2O_5/TiO_2. $[NH_3] = [NO] = 1000$ ppm, $O_2 = 2\%$, N_2 = balance, GHSV = 15,000 hr^{-1}, $T = 300°C$. (A) no pretreatment, (B) pretreatment at 650°C in dry O_2 for 2 hr, (C) same as in B with 2.2% H_2O in reactant.

Water is a reaction product in the SCR reaction. The rate of the reaction is not influenced by water vapor. The slow response to reach a steady state in run B indicated that the surface was dehydroxylated by the heat treatment and that the activity was restored by the accumulation of the OH groups by dissociation of the reaction product water. The addition of 2.2% H_2O in run C quickly provided the OH groups and hence the activity.

Only a small amount of the anatase support was transformed into rutile by the heat treatment. Saleh *et al.* (*19*) showed that 6% of the anatase was converted to rutile in a 7% V_2O_5/TiO_2 sample after heat treatment at 650°C. The presence of the small amount of rutile was apparently not enough to alter the structure of the supported V_2O_5, as indicated by the total restoration of the activity.

The results in Fig. 6 can also provide interesting information on the fraction of H_2O molecules produced by the reaction that is chemisorbed and retained on the same surface as OH and H. In the following calculation we assume the (010) plane is the only surface and, according to the model in Fig. 2, the OH and H are bonded to, respectively, the V_1 (or V_2) and O_1 sites. (Only V_1OH or V_2OH are active sites whereas O_1H is not an active site.) The initial (residual) activity in run B yielded 37% NO conversion. From the surface model, half of the V atoms can be occupied by OH groups. The amount of H_2O needed to restore the

activity in run B was 0.073 mmole. From the flow conditions (500 cm^3 NTP/min, 1000 ppm NO), the stoichiometry of the reaction, and the results for run B in Fig. 6, the following estimates can be obtained. During the initial 2-min period, 0.035 mmole H_2O was produced, whereas 0.033 mmole OH was needed to restore the activity to yield 67.5% NO conversion at t = 2 min. During t = 2–5 min, the amount of H_2O produced was 0.069 mmole, whereas 0.014 mmole OH was needed for the activity at t = 5 min (79.5% NO conversion). During t = 5–10 min, 0.133 mmole H_2O was produced, whereas 0.013 mmole OH was needed for the activity at t = 10 min (91% conversion). During t = 10–15 min, 0.149 mmole H_2O was produced, whereas 0.011 mmole OH was needed for the activity increase. The approximate efficiencies for chemisorbing H_2O as OH during the four time periods were 95%, 1 in 5, 1 in 10, and 1 in 13. This result indicates the energetic heterogeneity of the surface.

Active Sites and Poisoning Mechanism

The V=O group has been suggested as the active site for the SCR reaction and the activity of the catalyst has been suggested to be proportional to its density on the surface [e.g., (*2*)]. However, extensive evidence to the contrary has been shown and discussed in the literature (*8–10*). Moreover, correlation between IR/Raman spectra and SCR activity indicates that the V—OH groups are the active sites (*10, 11*).

Our results on poisoning by alkali metals, NH_3 chemisorption, IR, dehydroxylation, and EHMO calculation lead to the conclusion that the Brønsted acid sites of the V—OH groups (and specifically the terminal V—OH groups) are the active sites for the reaction. TiO_2 chemisorbs NH_3 by hydrogen bonding and Lewis acid site interactions (*37, 38*), but exhibits no SCR activity. The results of the alkali metal poisoning cannot be interpreted on the basis of V^{5+}=O being the active sites. XPS results (*39*) have shown that the addition of alkali metals to V_2O_5 stabilizes the 5+ valence. Thus, one would expect a promoting effect on the activity, which contrasts with the experimental results. The severity of poisoning by the alkali metals follows the basicity, which decreases the Brønsted acidity and hence the activity.

ACKNOWLEDGMENT

This work was supported by the Electric Power Research Institute.

REFERENCES

1. Bosch, H., and Janssen, F., *Catal. Today* **2,** 369 (1988).
2. Inomata, M., Miyamoto, A., and Murakami, Y., *J. Catal.* **62,** 140 (1980).
3. Miyamoto, A., Yamazaki, Y., Inomata, M., and Murakami, Y., *Chem. Lett. (Chem. Soc. Japan)*, 1355 (1978).
4. Miyamoto, A., Hattori, A., and Murakami, Y., *J. Solid State Chem.* **47,** 373 (1983).
5. Bosch, H., Janssen, F. J. J. G., Oldenziel, J., van den Kerkhof, F., van Ommen, J. G., and Ross, J. R. H., *Appl. Catal.* **25,** 239 (1986).
6. Janssen, F. J. J. G., van den Kerkhof, F. M. G., Bosch, H., and Ross, J. R. H., *J. Phys. Chem.* **91,** 5921 (1987).
7. Odriozola, J. A., Heinemann, H., Somorjai, G. A., Garcia de la Banda, J. F., and Pereira, P., *J. Catal.* **119,** 71 (1989).
8. Bond, G. C., Zurita, J. P., Flamerz, S., Gellings, P. J., Bosch, H., van Ommen, J. G., and Kip, B. J., *Appl. Catal.* **22,** 3610 (1986).
9. Gasior, M., Habor, J., Machej, T., and Czeppe, T., *J. Mol. Catal.* **43,** 359 (1988).
10. Rajadhyaksha, R. A., Hausinger, G., Zeilinger, H., Ramstetter, A., Schmelz, H., and Knözinger, H., *Appl. Catal.* **51,** 67 (1989).
11. Rajadhyaksha, R. A., and Knözinger, H., *Appl. Catal.* **51,** 81 (1989).
12. Takagi, M., Kawai, T., Soma, M., Onishi, T., and Tamaru, K., *J. Phys. Chem.* **80,** 430 (1976); *J. Catal.* **50,** 441 (1977).
13. Butt, J. B., and Petersen, E. E., "Activation, Deactivation and Poisoning of Catalysts," Academic Press, San Diego, CA/Orlando, FL, 1988.
14. Hegedus, L. L., and McCabe, R. W., "Catalyst Poisoning." Dekker, New York, 1984.
15. Yoshida, H., Takahashi, K., Sekiya, Y., Morikawa, S., and Kurita, S., *in* "Proceedings, 8th Congress on Catalysis, Berlin, 1988," Vol. 3, p. 649. Dechema, Frankfurt-am-Main, 1984.
16. Kasaoka, S., Sasaoka, E., and Nanba, H., *Nippon Kagaku Kaishi,* 486 (1984).

17. Shikada, T., and Fujimoto, K., *Chem. Lett. (Chem. Soc. Japan)*, 77; 515 (1983).
18. Baiker, A., Dollenmeier, P., and Glinski, M., *Appl. Catal.* **35,** 351 (1987).
19. Saleh, R. Y., Wachs, I. E., Chan, S. S., and Chersich, C. C., *J. Catal.* **98,** 102 (1986).
20. Yang, R. T., and Chen, J. P., *J. Catal.* **115,** 52 (1989).
21. Chen, J. P., and Yang, R. T., *Surf. Sci.* **21,** 481 (1989).
22. Vejux, A., and Cortine, P., *J. Solid State Chem.* **23,** 93 (1978).
23. Inomata, M., Miyamoto, A., and Murakami, Y., *J. Chem. Soc. Chem. Commun.*, 1009 (1979).
24. Murakami, Y., Inomata, M., Miyamoto, A., and Mori, K., *Stud. Surf. Sci. Catal.* **7,** 1344 (1981).
25. Suzuki, K., Hattori, T., Miyamoto, A., and Murakami, Y., *Chem. Lett. (Chem. Soc. Japan)*, 719 (1983).
26. Bystrom, A., Wilhelmi, K. A., and Brotzen, D., *Acta Chem. Scand.* **4,** 1119 (1950).
27. Enjalbert, R., and Galy, J., *Acta Crystallogr. Sect. C: Cryst. Struct. Commun.* **42,** 1467 (1986).
28. Pearson, W. B. (Ed.), "Structure report," Vol. 22, p. 282. Int. Union Crystallogr., Utrecht, 1968.
29. Pearson, W. B. (Ed.), "Structure report," Vol. 16, p. 212. Int. Union Crystallogr., Utrecht, 1959.
30. Jansen, I. M., and Wolf, B., *Z. Anorg. Chem.* **502,** 153 (1983).
31. Belokopytov, Y. V., Kholyavenko, V. M., and Geri, S. V., *J. Catal.* **60,** 1 (1979).
32. Kung, M. C., and Kung, H. H., *Catal. Rev.-Sci. Eng.* **27,** 425 (1985).
33. Matsuda, S., Kamo, T., Kato, A., Nakajima, F., Kumura, T., and Kurada, H., *Ind. Eng. Chem. Prod. Res. Dev.* **21,** 48 (1982).
34. Nam, I., Eldridge, J. W., and Kittrell, J. R., *Ind. Eng. Chem. Prod. Res. Dev.* **25,** 192 (1986).
35. Okazaki, S., Kuroha, H., and Okuyama, T., *Chem. Lett. (Chem. Soc. Japan)*, 45 (1985).
36. Tanabe, K., "Solid Acids and Bases." Academic Press, New York, 1970.
37. Primet, M., Pichat, P., and Mathieu, M., *J. Phys. Chem.* **75,** 1221 (1971).
38. Tsyganeko, A. A., Pozdnyakov, D. V., and Filimonov, V. N., *J. Mol. Struct.* **29,** 299 (1975).
39. Martin, C., Rives, V., and Gonzalez-Elipe, A. R., *J. Catal.* **114,** 473 (1988).
40. Murakami, Y., Inomata, M., Mori, K., Ui, T., Suzuki, K., Miyamoto, A., and Hattori, T., *in* "Preparation of Catalysts III" (P. G. Poncelet and P. A. Jacobs, Eds.), p. 531. Elsevier, Amsterdam, 1983.
41. Wong, W. C., and Nobe, K., *Ind. Eng. Chem. Prod. Res. Dev.* **25,** 179 (1986).